UC San Diego
UC San Diego Previously Published Works

Title

Crust-mantle interaction inferred from the petrology and Sr-Nd-Pb isotope geochemistry of Eocene arc lavas from the Kahrizak Mountains, north-central Iran

Permalink

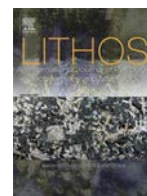**Authors**

Yazdani, Sima
Castillo, Paterno R
Hassanzadeh, Jamshid

Publication Date

DOI

Peer reviewed

Contents lists available at ScienceDirect

Lithos

Crust-mantle interaction inferred from the petrology and Sr-Nd-Pb isotope geochemistry of Eocene arc lavas from the Kahrizak Mountains, north-central Iran

Sima Yazdani [a,b,*], Paterno R. Castillo [a], Jamshid Hassanzadeh [c]

[a] *Scripps Institution of Oceanography, University of California, La Jolla, CA, USA*
[b] *School of Geology, College of Science, University of Tehran, Tehran, Iran*
[c] *Division of Geological and Planetary Sciences, California Institute of Technology, Pasadena, CA, USA*

ARTICLE INFO

ABSTRACT

The Eocene volcanic rocks from the Kahrizak Mountains in north-central Iran are part of the Urumieh-Dokhtar magmatic arc, which runs parallel to the Main Zagros Thrust segment of the Neo-Tethys suture. These volcanic rocks, similar to those from eastern Pontides and northern Anatolia, Turkey, were mainly produced during the Eocene magmatic flare-up associated with the Arabia-Eurasia convergence. The rock suite includes basalt, trachyandesite/andesite and trachydacite/rhyolite lavas and pyroclastic deposits that evolved compositionally from calc-alkalic to shoshonitic. Their normalized trace element concentration patterns are moderately enriched in light rare earth element and depleted in high field-strength elements (HFSE; e.g., Nb, Ta, Ti). They have narrow ranges of initial Pb isotopic ratios and $^{143}Nd/^{144}Nd_i$, but highly variable $^{87}Sr/^{86}Sr_i$. The new analyses indicate that the parental magmas of the volcanic rocks were derived from a mantle source that had been enriched by fluids released from a subducted oceanic slab. The fluids introduced significant amounts of large ion lithophile elements, but negligible HFSE to the source. The parental magmas underwent fractional crystallization and assimilation of upper crustal materials to produce the range of volcanic rocks. Integration of new analyses with regional data suggests that the Eocene volcanic rocks from north-central Iran, together with ~coeval volcanic rocks in eastern Pontides and northern Anatolia, were most probably derived from a lithospheric mantle source that had been previously metasomatized by fluids derived from a subducted slab before and during the Arabia-Eurasia collision.

© 2018 Elsevier B.V. All rights reserved.

1. Introduction

Magma genesis in subduction zones is generally more complex than in divergent plate boundaries and intraplate settings due to the wide range of igneous, sedimentary, metamorphic, and aqueous fluid components that potentially participate during the partial melting, magma mixing and assimilation processes that generate arc magma. The complexity is multiplied in continental margins because the ascent of magma through thick and compositionally heterogeneous overriding plate, combined with prolonged magma storage, bring about additional compositional modifications observed in continental arc magmas. Over the last two decades extensive investigations on crust-mantle interactions have been carried out for some of the major Cenozoic continental arc systems such as the Andes (e.g., Mattioli et al., 2006; Schiano et al., 2010), Indonesia (Gertisser and Keller, 2003) and Turkey (Temizel et al., 2012); however, modern detailed geochemical methods have seldom been applied to the Eocene arc of Iran.

In this paper we deal with a poorly investigated Eocene arc volcanic suite from the Kahrizak Mountains in north-central Iran in order to better constrain its tectono-magmatic evolution in the context of coeval magmatism in the region (Fig. 1). Eocene arc volcanism represents the most voluminous magmatic event in Iran, so much so that it has been ranked with famous flare-ups worldwide (Verdel et al., 2011). The volcanism is ultimately associated with the Neo-Tethyan plate subduction during the Mesozoic and Cenozoic (e.g., Deevsalar et al., 2017; Omrani et al., 2008; Verdel et al., 2011; Zhang et al., 2018). The Eocene arc volcanic suite from north-central Iran is compositionally diverse and includes mantle-derived mafic to crustal-contaminated felsic end-members, although some intermediate varieties are also present. In this contribution we focus on crust-mantle interactions by employing the petrography, mineral compositions, major and trace element

* Corresponding author at: Scripps Institution of Oceanography, University of California, La Jolla, CA, USA.

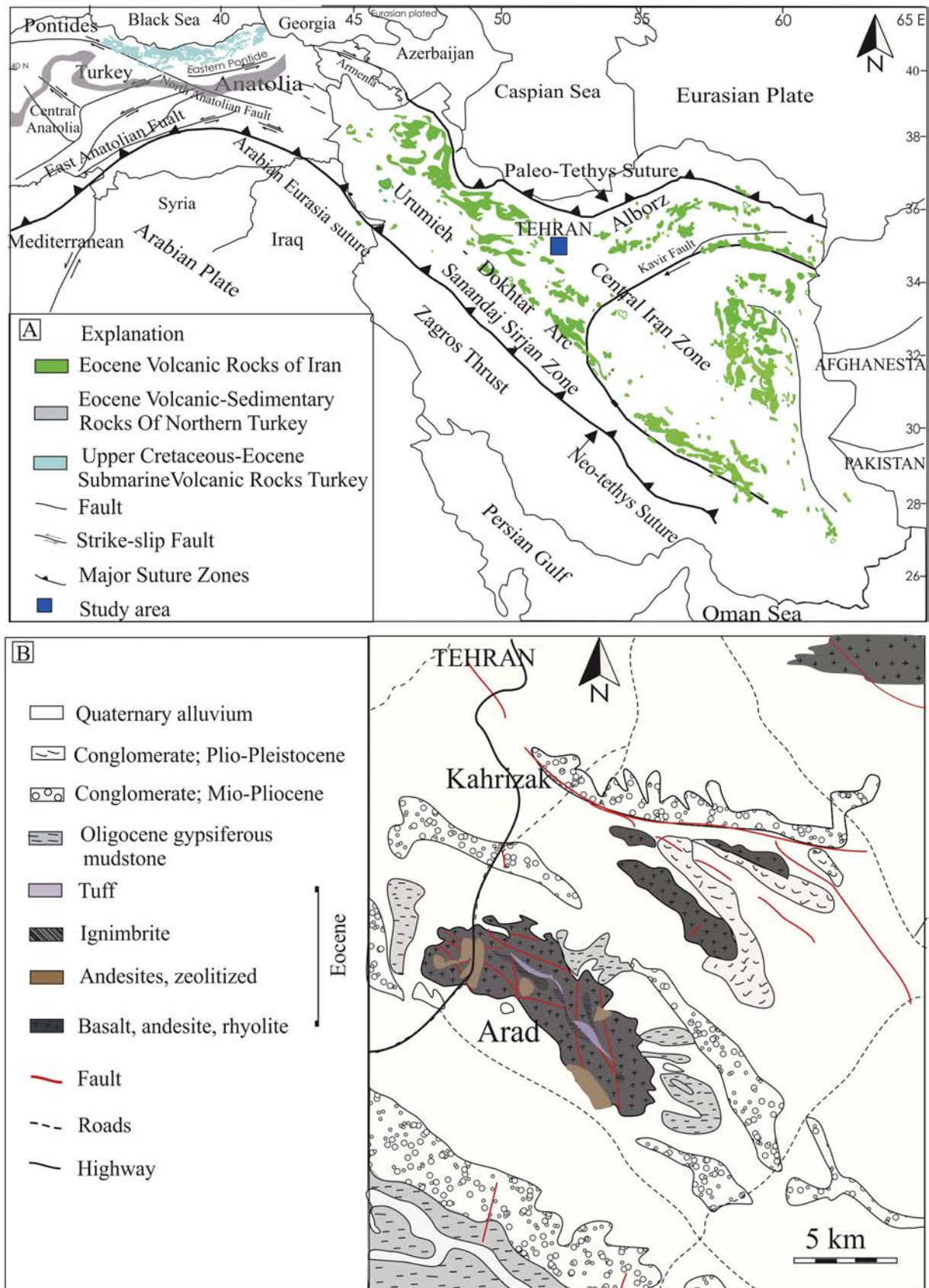*E-mail address:* siyazdan@ucsd.edu (S. Yazdani).

Fig. 1. (A) Simplified geological map of the Iran and Turkey region showing major sutures and continental blocks (modified after Kheirkhah et al., 2009; Whitechurch et al., 2013). The main Paleo-and Neo-Tethyan sutures are represented by heavy lines with filled triangles and the Eocene volcanic rocks in Iran by green areas (after Agard et al., 2011). Upper Cretaceous-Eocene volcanic rocks and Eocene volcanic-sedimentary successions along the Izmir-Ankara suture (Keskin et al., 2008) across Turkey are also shown. The location of study area is marked by the blue square south of Tehran. (B) Simplified geological map of the Kahrizak area (after Afaghi et al., 1986). (For interpretation of the references to colour in this figure legend, the reader is referred to the web version of this article.)

chemistry, and Sr, Nd and Pb radiogenic isotopes of the Eocene arc volcanic suite.

2. Geological setting and field relations

The substrate of the Iranian Paleogene arc consists of a mosaic of continental basement blocks that was consolidated during the Neoproterozoic-Early Cambrian Cadomian orogeny along the northern margin of Gondwana (Hassanzadeh et al., 2008; Rahmati-Ilkhchi et al., 2011; Ramezani and Tucker, 2003). The opening of Neo-Tethys Ocean in the Permian time left these basement blocks situated between a new ocean that was expanding and an older one that was being consumed (Berberian and King, 1981). The subduction initiation along the northern margin of the Neo-Tethys, beneath the Sanadaj-Sirjan zone of Iran, followed the collision between northern Iran and Eurasia during closing of the Paleo-Tethys (Berberian and Berberian, 1981; Hassanzadeh and Wernicke, 2016; Horton et al., 2008). In the Cretaceous-Paleocene time, arc magmatism diachronously shifted to the northeast and formed the Urumieh-Dokhtar zone in central Iran (Hosseini et al., 2017; Verdel et al., 2011).

The Kahrizak Mountains are located twelve miles south of Tehran in north-central Iran (Fig. 1). They are part of the Urumieh–Dokhtar arc (UDA) in the northern sector of the Central Iran tectonic province, which is bounded by the Sanandaj–Sirjan zone in the west-southwest, and by the Alborz Mountains in the north. To the east, the UDA includes the Great Kavir Depression, which is underlain by one of the aforementioned Gondwana basement blocks exposed in several tectonic windows, with igneous protoliths ranging in age from ca. 580 to 520 Ma (e.g., Hassanzadeh et al., 2008; Rahmati-Ilkhchi et al., 2011; Ramezani and Tucker, 2003). Sedimentary cover of the Great Kavir Block includes thick (≤9 km) Paleozoic-to-Cenozoic sequences that are largely comparable to those overlying the other basement blocks. Geochronological data obtained from the few outcrops of the Great Kavir Block additionally indicate granite-tonalite plutonic emplacement at ca. 215 Ma in the Saghand area (Ramezani and Tucker, 2003) and a medium-pressure amphibolite-facies metamorphism at ca. 166 Ma in the Rezveh area (Rahmati-Ilkhchi et al., 2011) to the southeast and east, respectively, of the Kahrizak Mountains.

Eocene calc-alkaline volcanic rocks occur almost throughout Central Iran and partly in neighboring provinces (Fig. 1; e.g., Verdel et al., 2011; Moghadam et al., 2016). Radiometric ages (U—Pb and $^{40}Ar/^{39}Ar$) of lava and pyroclastic samples from UDA and Alborz Mountains as well as mafic and silicic plutonic rocks from the Sabzevar, Khorram Darreh and Saghand areas in Central Iran and Sanandaj–Sirjan zone range from 55 to 37 Ma (Hassanzadeh et al., 2008; Moghadam et al., 2016; Ramezani and Tucker, 2003; Verdel et al., 2011). This magmatic flare-up occurred supposedly while the Neo-Tethyan slab began a slow roll-back after a subhorizontal subduction in the Late Cretaceous-Paleocene times (Verdel et al., 2011; Zhang et al., 2018; and references therein). The Eocene volcanic rocks were largely erupted in shallow marine environment, but concomitant basin and range tectonism also generated subaerial volcanic eruptions and rapid accumulations of thick sediments, volcano-sedimentary deposits, pyroclastics, and lava flows in the subsiding basins (Amidi et al., 1984). Volcanism diminished and the region began uplifting at the closure of the Neo-Tethys Ocean, and this was followed by the Arabia-Eurasia collision that is estimated to be in late Eocene (ca. 35 Ma - Bottrill et al., 2012), or late Oligocene (ca. 27 Ma, Pirouz et al., 2017). Deposition of detrital and shallow marine sediments with sparse volcanism ensued during the late Oligocene-early Miocene time and formed the conspicuous trio of Lower Red, Qom and Upper Red Formations indicating a broad subsidence sandwhiched between uplifts, most likely due to the dynamic topography of the overlying plate during continental collision (e.g., Bottrill et al., 2012). The Qom Formation is carbonate-dominant and thickest (500–1000 m) in central Iran, but extends into northwest Iran and southern Turkey with varying thicknesses.

The Eocene volcanic rocks exposed in the northern and eastern parts of the Kahrizak Mountains mainly consist of about 300 m of variegated rhyolites and dacitic to trachytic tuffs. These are overlain by ignimbrites that are mainly trachydacite in composition and are easily distinguished by their massive outcrops and steep slopes. Widespread distribution of acidic tuffs and ignimbrites suggests that the initial volcanic activity in the area was explosive. The explosive phase was followed by lava eruptions. In some parts of the study area, the pyroclastic rocks are overlain by a lesser volume of rhyolitic lavas. A ~130 m thick sequence of basalt and pyroxene-bearing basaltic andesite, basaltic trachyandesite and trachyandesite also occurs in the Kahrizak Mountains. Zeolites are common secondary minerals. The strata are dissected by several faults which are N- and NW-trending.

3. Analytical methods

>200 thin-sections of volcano-sedimentary rocks from various stratigraphic levels of the Kahrizak Mountains were analyzed under the microscope to identify their mineralogy and petrographic characteristics, and to select the least altered samples – i.e., those without veinlets and amygdales as well as secondary calcite, quartz, chlorite, zeolites, and/or clay minerals. Chemical compositions of minerals were determined using the JEOL 8200 electron microprobe at the California Institute of Technology using a focused electron beam with an accelerating voltage of 15 kV and a beam current of 25 nA. Standards for analysis were anorthite (SiKα, AlKα, CaKα); albite (NaKα); fayalite (FeKα); forsterite (MgKα); Mn_2SiO_4(MnKα); TiO_2(TiKα); Cr_2O_3(CrKα); and microcline (KKα). A precision approaching <1% relative error and accuracy as good as 1–2% were obtained. Quantitative elemental microanalyses were processed with the CITZAF correction procedure (Armstrong, 1995), and analytical results are given in supplementary Table S1.

Through petrographic inspections, 14 representative samples were selected as the least altered for determining whole rock compositions at the ACME Analytical Laboratories (Vancouver, Canada). Major element compositions were analyzed by inductively-coupled plasma-atomic emission spectrometry (ICP-AES). Trace elements, including rare earth elements (REE), were determined by inductively-coupled plasma-mass spectrometry (ICP-MS). The major and trace element compositions of two samples (K.91.31 and K.91.14) were analyzed at the Lab West Mineral Analysis LTD- Australia, and Zarazma Mineral Studies Co, Iran. The major and trace element analyses including their precisions are presented in Table 1 and supplementary Table S2.

Strontium, Nd and Pb isotope ratios for 9 of the samples were determined using a 9-collector, Micromass Sector 54 thermal ionization mass spectrometer (TIMS) at the Scripps Institution of Oceanography, University of California, San Diego. The sample preparation procedure used is similar to that described in Tian et al. (2008). Chips of whole rock samples were hand-picked to avoid fracture- and vug-filled portions as well as weathered crust, ultrasonicated in dilute HNO_3 acid for about 30 min, rinsed with ultrapure H_2O, and dried in an oven at 105 °C overnight prior to powdering in an alumina ceramic grinder. About 35 mg powder of each sample were digested with a double-distilled, 2:1 mixture of concentrated $HF:HNO_3$ acid in a clean Teflon beaker. Lead was first separated by re-dissolving the dried samples in 1 N HBr and then passing the solutions through a small ion exchange column in an HBr medium. Strontium and REE were separated from the residual solutions in an ion exchange column using HCl as the eluent. Finally, Nd was separated from the rest of the REE in an ion exchange column using alpha hydroxyisobutyric acid as the eluent. The isotopic analyses are presented in Table 2, which also includes the details of the TIMS procedure as footnotes.

Table 1
Major and trace element contents of representative volcanic rocks from the Kahrizak Mountains, north-central Iran.

Sample	K.91.14	K.91.31	K.B.3	K.E.30	K.EL.1	K.ET.5	K.S.18"	K.SH.21	K.Y.10	S0–19	+/−[a]
SiO_2 (wt%)	68.35	67.40	50.11	57.03	70.00	50.45	58.65	49.50	72.56	61.13	0.88
TiO_2	0.47	0.33	1.06	1.44	0.78	1.13	0.90	1.23	0.39	0.69	0.01
Al_2O_3	15.41	16.18	17.29	16.39	14.84	18.47	18.43	19.23	14.18	13.95	0.28
Fe_2O_3	2.14	1.40	3.95	3.96	2.18	4.00	3.15	4.11	1.33	7.47	0.16
MnO	0.08	0.08	0.15	0.10	0.13	0.15	0.07	0.14	0.05	0.13	0.01
MgO	0.56	0.20	6.73	2.60	0.09	4.62	2.27	4.21	0.63	2.88	0.08
CaO	1.36	3.42	9.72	6.17	0.34	10.23	4.65	10.23	2.36	6.00	0.16
Na_2O	3.58	4.78	2.58	3.54	1.85	2.89	4.71	2.88	3.75	4.11	0.23
K_2O	6.49	5.06	1.33	3.07	8.07	1.18	3.41	1.36	3.52	1.29	0.07
P_2O_5	0.11	0.15	0.33	0.82	0.15	0.34	0.59	0.35	0.09	0.32	0.01
LOI	2.32	2.58	2.90	2.50	4.40	2.50	3.10	3.10	4.40	1.94	
Total	100.05	100.02	99.99	99.98	99.95	99.99	99.99	99.96	100.00	99.91	
Sc (ppm)	5.00	7.00	29.00	20.00	11.00	30.00	10.00	29.00	6.00	27.00	1.10
V	36.0	31.0	264	181	19.0	284	64.0	307	29.0	165	19.0
Co	4.10	3.70	48.10	27.30	22.50	43.20	20.00	43.20	17.90	24.00	2.00
Ni	3.00	2.00	32.90	1.50	0.30	13.00	0.30	15.30	0.50	470.00	44.00
Rb	161	141	26.4	89.5	194	21.9	78.3	30.2	143	19.5	1.80
Sr	68.4	198	603	559	77.8	660	587	690	407	317	30.0
Zr	60.0	95.0	70.3	197	252	87.3	199	85.3	191	112	9.2
Nb	12.70	13.30	5.50	15.20	19.00	6.60	15.90	7.70	11.90	69.00	8.00
Cs	2.60	2.20	1.00	1.80	1.20	0.30	1.00	0.30	48.00	4.50	0.30
Ba	887	759	382	694	675	338	788	320	697	486	20
La	39.80	32.40	15.70	37.80	35.10	16.70	37.30	16.70	26.90	71.30	5.80
Ce	70.70	55.30	32.40	81.20	76.90	36.20	77.50	36.00	50.80	161.00	8.40
Pr	7.79	6.22	3.92	9.39	8.46	4.32	8.82	4.50	5.23	19.40	1.40
Nd	26.80	22.70	16.80	39.40	31.90	17.90	35.10	19.80	19.40	75.70	6.40
Sm	5.39	4.26	4.50	8.70	6.90	4.10	7.50	4.70	3.70	13.70	1.00
Eu	0.87	1.02	1.32	2.25	1.37	1.33	1.99	1.54	0.74	3.81	0.24
Gd	4.94	4.32	4.16	8.55	5.94	4.43	6.67	4.50	3.37	10.53	0.78
Tb	0.65	0.65	0.68	1.26	0.98	0.61	0.94	0.69	0.60	1.41	0.08
Dy	3.60	3.73	3.84	7.37	5.99	4.09	5.57	4.20	3.27	7.50	0.38
Ho	0.76	0.81	0.74	1.36	1.24	0.77	1.07	78.00	0.66	1.39	0.17
Er	2.23	2.42	2.06	3.94	3.69	2.21	3.30	2.34	2.02	3.78	0.48
Tm	0.45	0.41	0.30	0.60	0.57	0.31	0.48	0.32	0.33	0.55	0.05
Yb	2.74	2.75	1.92	3.83	4.05	2.15	3.25	2.34	2.37	3.55	0.17
Lu	0.46	0.43	0.28	0.59	0.62	0.32	0.54	0.34	0.40	0.53	0.04
Hf	1.86	2.51	1.90	5.50	8.10	2.60	5.00	2.40	5.40	3.10	0.13
Ta	0.85	0.75	0.40	1.10	1.40	0.40	0.90	0.50	1.00	4.90	0.60
Pb	5.80	16.10	1.60	3.70	13.40	2.20	5.80	3.00	6.80	–	–
Th	20.8	15.30	2.00	8.50	15.00	2.40	5.40	1.90	12.80	13.00	1.10
U	3.60	3.34	0.60	2.40	4.00	0.70	1.60	0.60	4.80	19.40	2.40

[a] at 95% confidence interval. Additional information on accuracy and precision can be found at www.acmelab.com.

4. Results

4.1. Petrography and mineral chemistry

The bulk compositions of the Eocene lava flows and pyroclastic rocks from the Kahrizak Mountains range from basalt to rhyolite. Based on their mineralogy and major element composition, these rocks generally belong to two main groups, calc-alkaline basaltic and alkaline trachydacite-rhyolite groups (Fig. 2). The pyroclastic rocks include tuff and ignimbrite and are widespread in the area. Below we present the results of our investigation of each compositional group.

Table 2
Sr, Nd and Pb isotopic ratios of volcanic rocks from the Kahrizak Mountains, north-central Iran.

Sample name	$^{87}Sr/^{86}Sr$	$(^{87}Sr/^{86}Sr)i$	$^{143}Nd/^{144}Nd$	$(^{143}Nd/^{144}Nd)i$	εNd	$^{206}Pb/^{204}Pb$	$(^{206}Pb/^{204}Pb)i$	$^{207}Pb/^{204}Pb$	$(^{207}Pb/^{204}Pb)i$	$^{208}Pb/^{204}Pb$	$(^{208}Pb/^{204}Pb)i$
K.ET.5	0.707449	0.707285	0.512689	0.512580	−0.12	18.758	18.636	15.623	15.605	38.781	38.367
K.SH.21	0.705103	0.704887	0.512687	0.512574	−0.24	18.603	18.526	15.589	15.578	38.593	38.277
K.E.30	0.705346	0.704557	0.512671	0.512566	−0.41	18.680	18.431	15.605	15.569	38.704	37.832
K.EL.1	0.704970	0.692648	0.512686	0.512583	−0.06	18.551	18.436	15.550	15.533	38.489	38.064
K.91.31	0.706618	0.703106	0.512720	0.512631	0.87	18.713	18.633	15.628	15.616	38.741	38.380
K.91.14	0.707945	0.696337	0.512718	0.512623	0.70	18.926	18.688	15.650	15.615	39.009	37.647
K.S.18"	0.705215	0.704557	0.512692	0.512591	0.08	18.606	18.500	15.610	15.595	38.647	38.293
K.B.3	0.704916	0.704700	0.512699	0.512572	−0.29	18.616	18.472	15.610	15.589	38.681	38.206
K.Y.10	0.706195	0.704463	0.512729	0.512639	1.01	18.733	18.462	15.633	15.593	38.784	38.069

Strontium, Nd and Pb isotope ratios were analyzed using a 9-collector, Micromass Sector 54 thermal ionization mass spectrometer (TIMS). Total procedural blanks are 35 pg for Sr, 10 pg for Nd and 60 pg for Pb. Strontium isotopic ratios were fractionation-corrected to $^{86}Sr/^{88}Sr = 0.1194$ and are reported relative to $^{87}Sr/^{86}Sr = 0.710254 \pm 0.000018$ (n = 22) for NBS 987 during the period of analysis. Neodymium isotopic ratios were measured in oxide form, fractionation corrected to $^{146}NdO/^{144}NdO = 0.72225$ ($^{146}Nd/^{144}Nd = 0.7219$) and are reported relative to $^{143}Nd/^{144}Nd = 0.511856 +/− 0.000016$ (n = 19) for the La Jolla Nd Standard during the period of analysis. Lead isotopic ratios were analyzed using the double-spike method to correct for mass fractionation during analyses; separate measurements of spiked and unspiked samples were made on different aliquots from the same dissolution. The SBL-74 ^{207}Pb −^{204}Pb double-spike from the University of Southampton was used. During the analysis period, the method produced the following results for NBS981: $^{206}Pb/^{204}Pb = 16.930 \pm 0.002$, $^{207}Pb/^{204}Pb = 15.490 \pm 0.003$ and $^{208}Pb/^{204}Pb = 36.700 \pm 0.009$ (n = 11). 2σ precisions for individual runs are better than these.
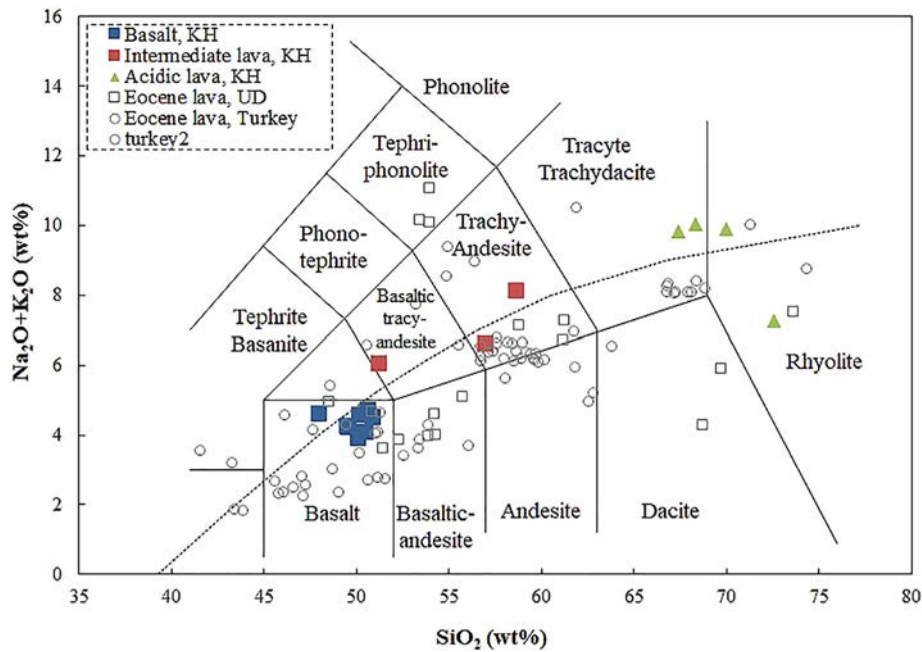
Fig. 2. Total alkali versus silica classification diagram (Le Bas et al., 1986) for the Kahrizak (KH) volcanic rocks. The volcanic rocks generally plot along the alkaline-subalkaline divide of Irvine and Baragar (1971). Also plotted for reference are Eocene volcanic rocks from Urumieh-Dokhtar (UD) (Omrani et al., 2008; Verdel et al., 2011), Eocene volcanic rocks from Sabzevar (SZ) (Moghadam et al., 2016) and Turkey (eastern Pontides - Aydıncakır and Sen, 2013; Temizel et al., 2012 and northern Anatolia - Keskin et al., 2008).

4.1.1. The calc-alkaline basaltic group

This group is commonly observed closely together in the field and includes basalt and intermediate rocks including basaltic trachyandesite, trachyandesite and andesite. The basalts show a wide range of textures, from phyric, microphyric, hyalophyric, glomerophyric to rarely intersertal, intergranular, and trachytic. Their typical mineral assemblages include plagioclase, olivine, clinopyroxene, orthopyroxene, and Fe—Ti oxide (Table S1 and Fig. 3A-F). Plagioclase ($Na_{0.10-0.51}Ca_{0.29-0.92}Si_{0.20-3.03}Al_{0.77-1.95}O_8$) ranges from labradorite to bytownite in composition (An$_{55-90}$;Figs. 4A, B). Plagioclase phenocrysts generally exhibit oscillatory zoning and sieve texture (Fig. 3A-C); some have reaction rims and are rounded. Those with oscillatory zoning generally have bytownite to anorthite cores and albite (An$_{25.9}$) and andesine (An$_{35.7-45.9}$) rims (Fig. 4C). Some basalts have phenocrysts with andesine rim and oligoclase (An$_{26.4-32.4}$) core; others show crystals of Na-sanidine ($K_{0.22}Na_{0.24}Al_{0.53}Si_{1.46}O_8$) in the cores of oligoclase.

Olivine occurs as euhedral to subhedral crystal, range from chrysolite ($Fe_{0.19-0.20}Mg_{0.46-0.51}Si_{1.18-1.23}O_4$) to hyalosiderite ($Fe_{0.19-0.29}Mg_{0.44-0.49}Si_{1.17-1.75}O_4$) in composition (Fig. 4E) and appears to be zoned. Clinopyroxene ($Wo_{43-49}En_{37-43}Fs_{13-16}$) occurs as euhedral to subhedral grains and is diopside-augite in composition ($Na_{0.03-0.63}Ca_{0.26-1.17}Fe_{0.04-0.04}Mg_{0.03-1.12}Al_{1.13-1.18}Ti_{0.01-0.04}Si_{2.41-2.58}O_6$) (Fig. 4D). Clinopyroxene also displays zonation and reaction textures with more sodic ($Wo_{79}En_{10}Fs_{11}$) rim composition (Fig. 4d, F). The Fe—Ti oxides are mainly magnetite-titanomagnetite ($Ti_{0.33-0.37}Fe_{2.37-2.57}O_4$) (Table S1).

The trachyandesites and basaltic trachyandesites consist mainly of plagioclase, clinopyroxene, hornblende, biotite, and Fe—Ti oxide. Plagioclase (An$_{36-59}$) (Fig. 4A and Table S1) occurs as euhedral to subhedral crystals and typically shows sieve texture and normal zoning. Hornblende occurs as subhedral grains and is classified (Hawthorne, 1983) as magnesio-hastingsite and magnesian hastingsite ($Na_{0.68-0.72}Ca_{1.71-1.73}Fe_{1.51-1.54}Si_{5.86-5.95}Al_{1.94-2.0}O_2(OH)_2$; magnesian number (Mg#) = 0.65–0.70) (Fig. 4F and Table S1).

The basaltic rocks were strongly affected by fluid/rock interaction and, thus, contain secondary minerals due to alteration. The paragenetic sequence of alteration began with precipitation of phyllosilicates on walls of veins followed by crystallization of Na-zeolite minerals (analcime, tetranatrolite and natrolite) and Ca-zeolites (thomsonite/natrolite, gonnardite, chabazite, stilbite, scolecite/mesolite, and heulandite) from the fluid. The latter is a mixture of sea and magmatic waters (Yazdani et al., 2014). The major-trace element and isotopic composition of zeolites and host rocks suggests that the alteration occurred penecontemporaneously with volcanic eruptions in a submarine environment.

4.1.2. The alkaline trachydacite-rhyolite group

This group includes rhyolite lavas, trachydacitic ignimbrites and tuffs. The mineral assemblage in rhyolites includes plagioclase, quartz and biotite in a glassy, trachytic groundmass. There are two varieties of glassy groundmass - dark brown and yellow. The rhyolites generally exhibit hyalo-microlitic porphyritic and spherulitic textures with perlitic cracks. Some quartz and many biotite grains have corroded rims. Ignimbrites vary in texture from vitrophyric to eutaxitic; the fiamme-bearing ignimbrites show vitroclastic and fluidal structures, in which the lenticular flames and phenocrysts are oriented along the flow direction. Tuffs of rhyolitic to dacitic composition consist of vitric, crystal and lithic tuffs.

4.2. Major and trace element compositions

The samples analyzed are mainly lava flows and two samples of pyroclastic rocks - an ignimbrite and a tuff. Notably, the analyses were done on samples that are petrographically the least altered. Hence, the chemical and isotope analytical results are considered a reflection of the primary composition of the volcanic rocks in the following discussion, unless noted otherwise.

The Kahrizak volcanic rocks display a large range of composition, with SiO_2 contents ranging from 48 to 73 wt% and Mg# of the basaltic rocks ranging from 30 to 43 (Tables 1 and S2). They range from basalt, basaltic trachyandesite, trachyandesite, to rhyolite (Fig. 2; Le Bas et al., 1986). The basaltic and andesitic rocks tend to be calc-alkaline to high-K calc-alkaline whereas the rhyolite and trachydacitic rocks tend to be high-K calc-alkaline to shoshonitic (Pecerillo and Taylor, 1976). According to the classification of Draper and Johnston (1992), the basalts are high-alumina and low magnesian ($SiO_2 = 48$–51 wt%; Al_2O_3
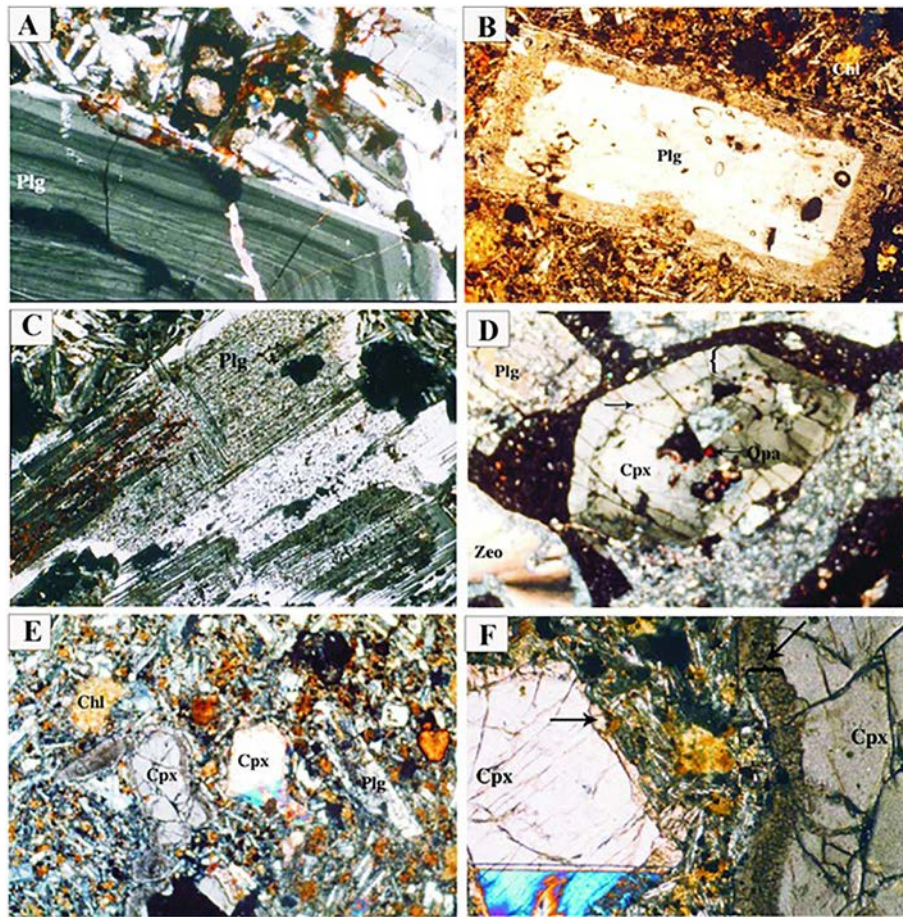
Fig. 3. Photomicrographs of the Kahrizak volcanic rocks displaying some of their textures and mineralogy. (A) Zoning of plagioclase in basalt; (B) and (C) plagioclase sieve texture in andesite; (D), (E), and (F) zoning and reaction rim (marked with arrows) in clinopyroxenes in andesitic-basalt and basalt, respectively. Abbreviations: Cpx: clinopyroxene; Plg: plagioclase; Zeo: zeolite; Opa: opaque; Chl: chlorite.

= 17–21 wt%; MgO = 4–7 wt%; CaO = 7.5–11 wt%). The samples generally exhibit negative CaO, MgO, Al_2O_3, FeO_t, TiO_2, Ni, Sr, and Co correlations, but positive K_2O, Ba, and Th correlations with SiO_2 (Fig. 5). All these variations are consistent with fractionation of the observed mineral phases olivine + clinopyroxene + plagioclase ± hornblende ± titanomagnete ± apatite in the volcanic rocks.

Relative to normal mid-ocean ridge basalts (MORB; Sun and McDonough, 1989), the samples show selective enrichments in large-ion lithophile elements (LILE; e.g., Sr, K, Rb, Ba, Th) and to a lesser extent in La and Ce, but depletions in some high field-strength elements (HFSE) such as Ta, Nb, Zr, and Hf (Fig. 6A). In general, the Kahrizak Mountains volcanic rocks and some Eocene arc volcanic rocks from the UDA (Omrani et al., 2008), eastern Pontides and northern Anatolia show similar trace element concentration patterns.

The volcanic rocks are moderately enriched in light REE (Fig. 6B). That is, the samples show moderately fractionated, subparallel REE concentration patterns (La/Lu_{Ch} = 4–11), indicating they may have come from a common, or at least, similar sources. Their REE concentrations increase with increasing differentiation from basalts to rhyolites. Moreover, the rhyolitic rocks display moderate negative Eu-anomalies (mean Eu_{Ch}/Eu^* = 0.512–0.726), suggesting plagioclase fractionation.

4.3. Pb, Nd and Sr isotopic ratios

The samples analyzed show a limited range of Pb isotopic values ($^{206}Pb/^{204}Pb_i$ = 18.431–18.688, $^{207}Pb/^{204}Pb_i$ = 15.533–15.616, and $^{208}Pb/^{204}Pb_i$ = 37.647–38.380; Table 2; Fig. 7A, B). In general, they appear to define linear arrays in Pb–Pb isotopic diagrams that either overlap and/or are parallel with the linear Pb isotopic fields of other Eocene lavas from Iran and of Tethyan basalts. The samples also have a narrow range of $^{143}Nd/^{144}Nd_i$ (0.51257–0.51264) but their $^{87}Sr/^{86}Sr_i$ (0.69265–0.70729) are heterogeneous and include usually low values, clearly indicating seawater alteration (Rossel et al., 2014) and/or upper crustal assimilation (Alagna et al., 2010). Thus, a number of what were selected as the least altered samples may have also been variably affected by either alteration or assimilation, or both. In general, however, the $^{87}Sr/^{86}Sr_i$ and $^{143}Nd/^{144}Nd_i$ of the bulk of basaltic and intermediate samples are lower than the majority of Eocene lavas from Iran and Turkey, but overlap with the Eocene high-Ti gabbros from the Sanandaj–Sirjan zone in western Iran that also have low $^{143}Nd/^{144}Nd_i$ and highly variable $^{87}Sr/^{86}Sr_i$ (Fig. 7C).

Another significant feature of Kahrizak volcanic rocks is their measured Pb isotopic ratios, best exemplified by $^{207}Pb/^{204}Pb$, generally increase with increasing SiO_2, i.e., from basalt to trachyandesite and pyroclastic rocks (Fig. 8A). Their measured $^{143}Nd/^{144}Nd$ and $^{87}Sr/^{86}Sr$ also increase with increasing SiO_2 (Fig. 8B, C).

5. Discussion

The Kahrizak volcanic rocks lack primitive rocks with Mg# > 70 and high compatible element abundances, e.g., Ni > 200 ppm, Cr > 400 ppm, that can be considered to represent magmas derived directly from peridotitic mantle (e.g., Tatsumi and Eggins, 1995). However, the Kahrizak volcanic rocks have similar initial Pb and Nd isotopic ratios, clearly indicating their cogenetic nature. Thus, before discussing the magma
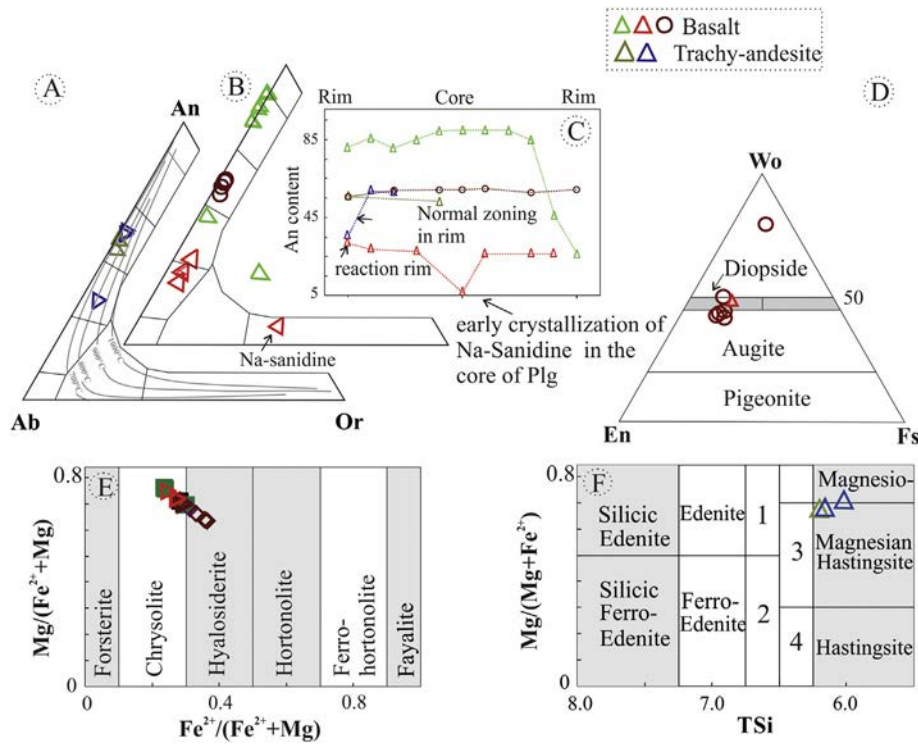
Fig. 4. (A, B) An-Ab-Or triangular plots showing the composition of feldspars in the Kahrizak volcanic rocks. The temperature curves are from Elkins and Grove (1990). Note that some of the plagioclases plot on curves that partially melt as high as 900 °C. (C) Anorthite content of the plagioclases plotted against distance from the core. (D) Clinopyroxene (Morimoto, 1988), (E) olivine and (F) hornblende (Hawthorne, 1983)classification diagrams for the Kahrizak volcanic rocks. In Fig. 4E: 1 = edenitic hornblende; 2 = ferro-edenitic hornblende; 3 = magnesian hastingsitic hornblende; 4 = hastingsitic hornblende.

genesis and source composition of these volcanic rocks, we first examine whether they are related to one another by fractional crystallization, crustal assimilation, or a combination of both (AFC), and magma mixing.

5.1. Assimilation-fractional crystallization (AFC)

As noted earlier, major and trace element variations of the analyzed volcanic rocks are consistent with crystal fractionation from a common or very similar parental magmas. Specifically, the observed major and trace element variations (Fig. 5) are consistent with fractionation of olivine + clinopyroxene + plagioclase ± hornblende ± titanomagnetite in the basalts, plagioclase + hornblende + clinopyroxene ± titanomagnetite in the andesites, and plagioclase + quartz + biotite ± hornblende ± sanidine ± titanomagnetite ± apatite in the rhyolites and trachydacites. In rhyolitic samples, negative Eu anomalies are indicative of feldspar removal during fractionation. However, such an anomaly is not present in the basalts. This observation, together with high Al_2O_3 and Ba contents and low La/Sr ratio (0.02–0.04), rule out any significant plagioclase fractionation in the basalts (Mattioli et al., 2006). On the other hand, in addition to their negative Eu anomalies (Fig. 6B), the Sr contents of the rhyolitic and pyroclastic rocks decrease with increasing SiO_2 (Fig. 5) and $^{87}Sr/^{86}Sr$ (not shown). These compositional features indicate the importance of plagioclase fractionation in the magmatic evolution of rhyolitic samples as the plagioclase partition coefficient for Sr is 1.8 in felsic rocks, but 0.1 for other trace elements (James, 1982). Moreover, the rhyolitic rocks are significantly low in P_2O_5 and TiO_2 relative to the basaltic rocks, indicating the potential roles of apatite and Fe—Ti oxide fractionation.

Significantly, the increase in REE concentrations of Kahrizak volcanic rocks from basalts to rhyolites (Fig. 6B) is accompanied by a decrease in Dy/Dy* values, which are a measure of the concavity of a REE pattern (Davidson et al., 2013). All samples have Dy/Dy* <1.0, or have concave up REE patterns; Dy/Dy* together with Dy/Yb decrease with differentiation (not shown), indicating that amphibole is a dominant

fractionating phase as well (Davidson et al., 2013). This is significant because the Sr/Y ratios of the Kahrizak volcanic rocks are as high as 76 in the basalts. Although a Sr/Y of 76 is still low compared to those of 'adakites' that are purported to be melts from subducted oceanic basalts at high pressure where garnet is stable (e.g., Castillo, 2012), they overlap with adakitic lavas from Iran and Turkey, some of which have indeed been proposed as partial melts of subducted basaltic crust (e.g., Ghorbani and Bezenjani, 2011). Combined with their relatively low La/Yb$_N$ values (≤10), the relatively high Sr/Y of Kahrizak basalts is most probably not due to partial melting of subducted basalt, but is also an indication of hornblende fractionation from parental hydrous magmas (e.g., Castillo et al., 1999; Moghadam et al., 2016).

Many studies on the evolution of arc magmas have shown that assimilation of crustal material is an important process to modify the trace element and isotopic composition of mantle-derived magmas (e.g., Schiano et al., 2010). For example, contamination of primary magmas by mature and thickened paleo-arc crust was proposed to be an important factor in the collisional and post-collisional Tertiary magma evolution in north-central Turkey (Temizel et al., 2012). Magma mixing is also important. For instance, Amidi et al. (1984) have argued that mixing of basaltic and palingenetic felsic magmas was responsible for producing the calc-alkaline Eocene volcanic rocks in Central Iran. Therefore, it is essential to evaluate the effects of crustal contamination on mantle-derived magmas, e.g., through mixing of mantle- and crustal-derived melts, on the composition of the Kahrizak volcanic rocks.

It is noteworthy that the trace element composition of bulk continental crust is quite similar to the composition of typical arc magmas. Thus, some of the major compositional features of crustal contamination are similar to, or hard to distinguish from, those of arc magmas derived from a mantle source metasomatized by aqueous fluids and/or melts derived from a subducted basaltic crust and overlying sediments (Verdel et al., 2011). As mentioned earlier, however, the Kahrizak volcanic rocks show evidence of mineral-melt
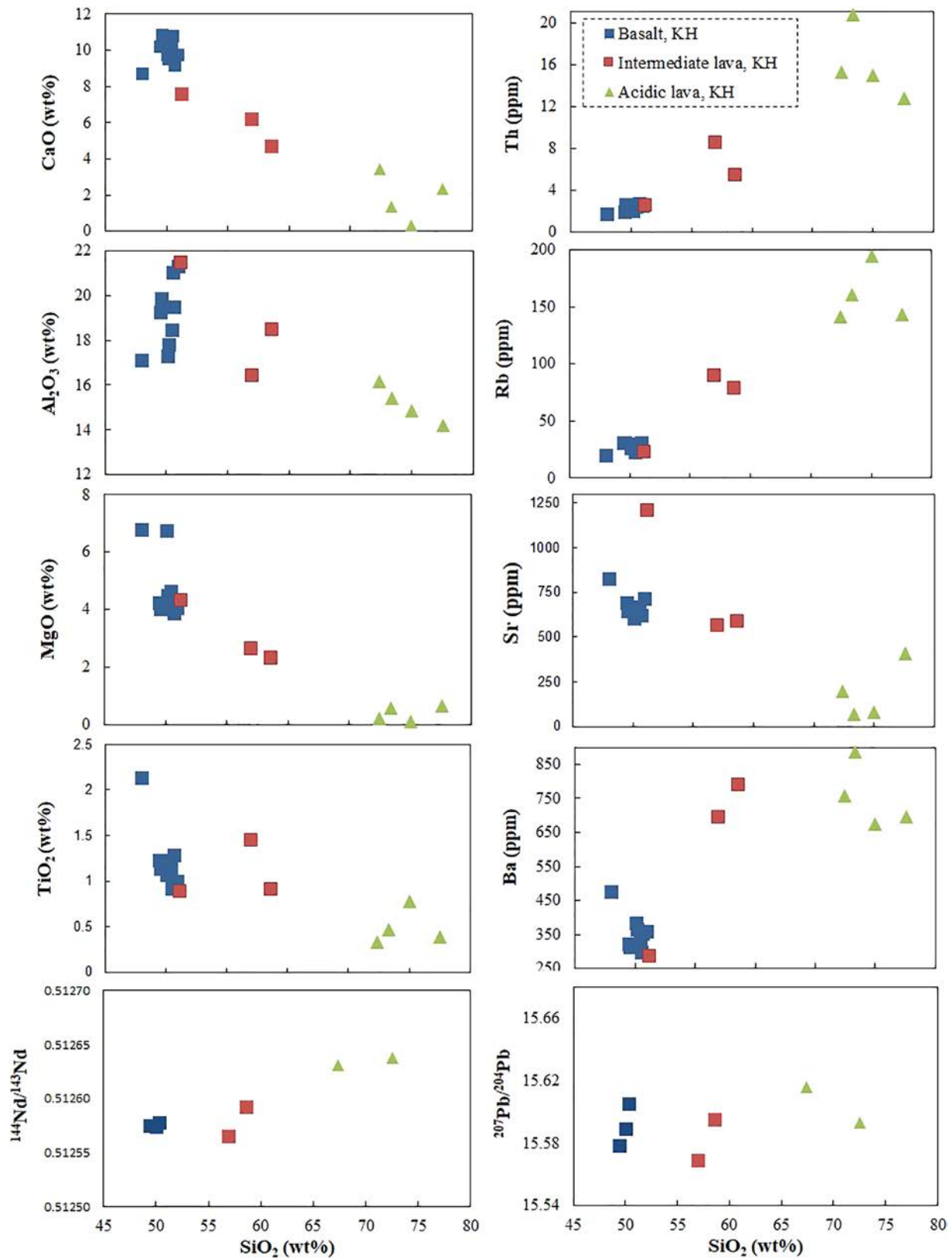
Fig. 5. SiO$_2$ (wt%) versus major oxide (wt%) and select trace elements (ppm) variation plots for the Kahrizak volcanic rocks. See text for discussion.

disequilibria including (1) Ca-rich plagioclase phenocrysts that exhibit oscillatory zoning and are rimmed with highly sodic plagioclase, sieve texture, corroded and rounded crystals, and early crystallization of Na-sanidine in the cores of oligoclase (Fig. 3A-C); (2) zoning and reaction rims in olivine phenocrysts; and (3) partial melting and

reaction rim in clinopyroxenes (Fig. 3D-F). These textures are usually interpreted as a result of magma mixing (Tsuchiyama, 1985) although they may also be due to rapid decompression, where heat loss is minor relative to ascent rate (Nelson and Montana, 1992). Disequilibrium textures in zoned pyroxene phenocrysts may also be the
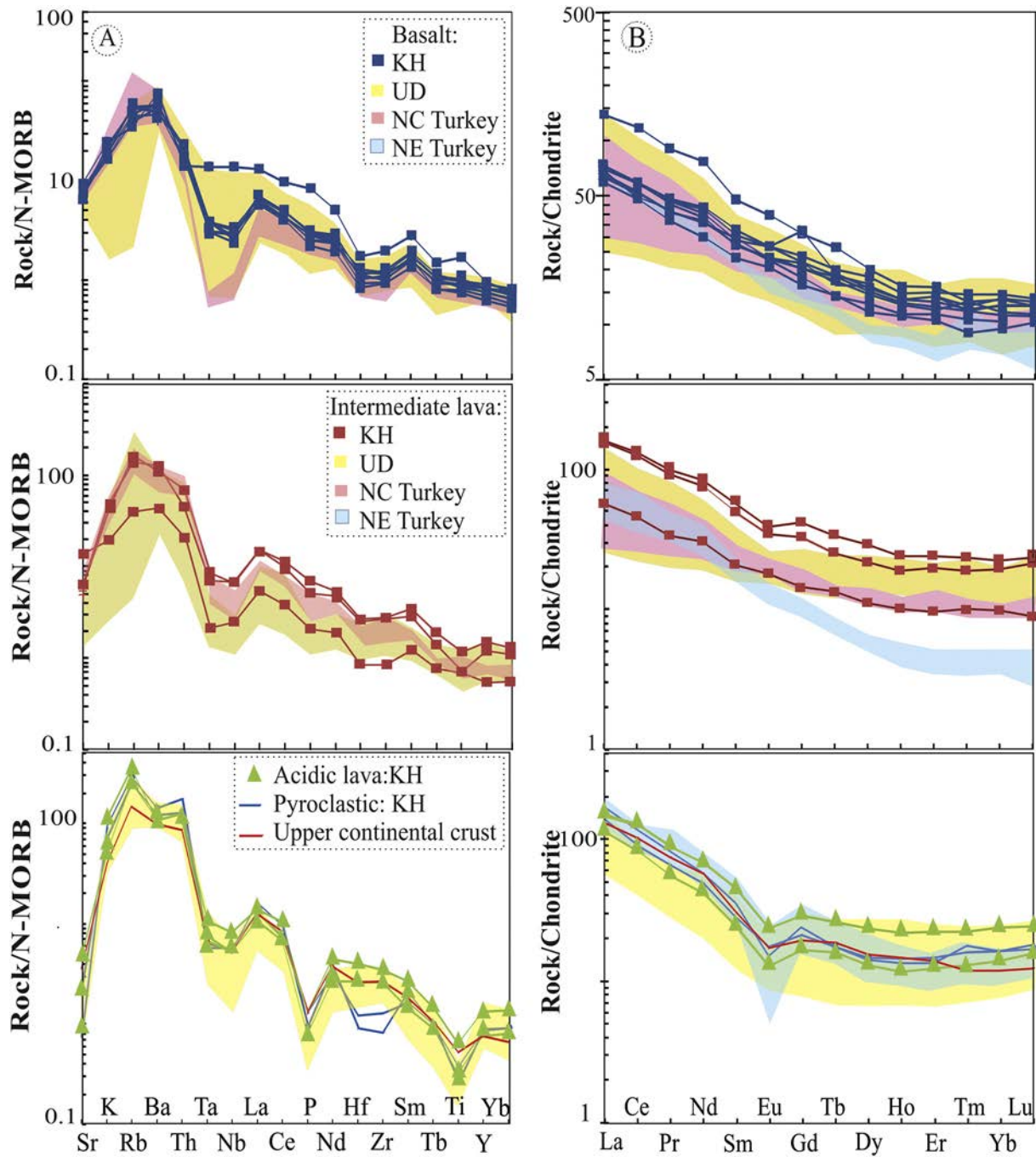
Fig. 6. (A) Normal-MORB normalized multi-element and (B) chondrite-normalized REE spider diagrams for the Kahrizak volcanic rocks (normalizing values are from Sun and McDonough, 1989). The upper continental crust (Rudnick and Gao, 2003) is plotted for comparison. Eocene volcanic rocks from eastern Pontides (NE) and northern Anatolia (NC) in Turkey are from Temizel et al. (2012) and Keskin et al. (2008), respectively.

results of assimilation of continental crust, rapid fall of H_2O pressure or magma mixing (Sakuyama, 1979).

Many volcanic systems most probably experience rapid decompression and reduction in pressure is a simpler mechanism to produce the above-mentioned disequilibrium textures as it requires no addition of heat or mass. Rapid decompression may also operate in conjunction with magma mixing because magmas generally decompress as they ascend. Thus, some of the observed variations in incompatible elements (e.g., enrichments of K, Rb, and Ba) may have been the result of crustal assimilation and/or mixing (Fig. 5). Note that although most of these elements are fluid-mobile and, thus, their enrichments could be attributed to recent low temperature alteration, we reiterate that petrographic and zeolite data indicate the

alteration and volcanic eruptions were penecontemporaneously in a submarine environment. Moreover, Rb/Sr and Rb generally increase with measured $^{87}Sr/^{86}Sr$ from basalt to rhyolite and trachydacite (Fig. 8D, E). As noted earlier, the Kahrizak volcanic rocks also display roughly positive correlations between measured radiogenic isotopes and SiO_2 (Fig. 8A-C). As these ca. 40 Myr old volcanic rocks are neither temporally nor spatially stratified, and can be traced back to a common or very similar sources, the observed isotopic and trace element versus isotopic relationships of the bulk of the analyses most likely are not the result of alteration. Instead, these relationships indicate that crustal assimilation, in addition to fractional crystallization, was involved in the petrogenesis of the Kahrizak volcanic rocks.
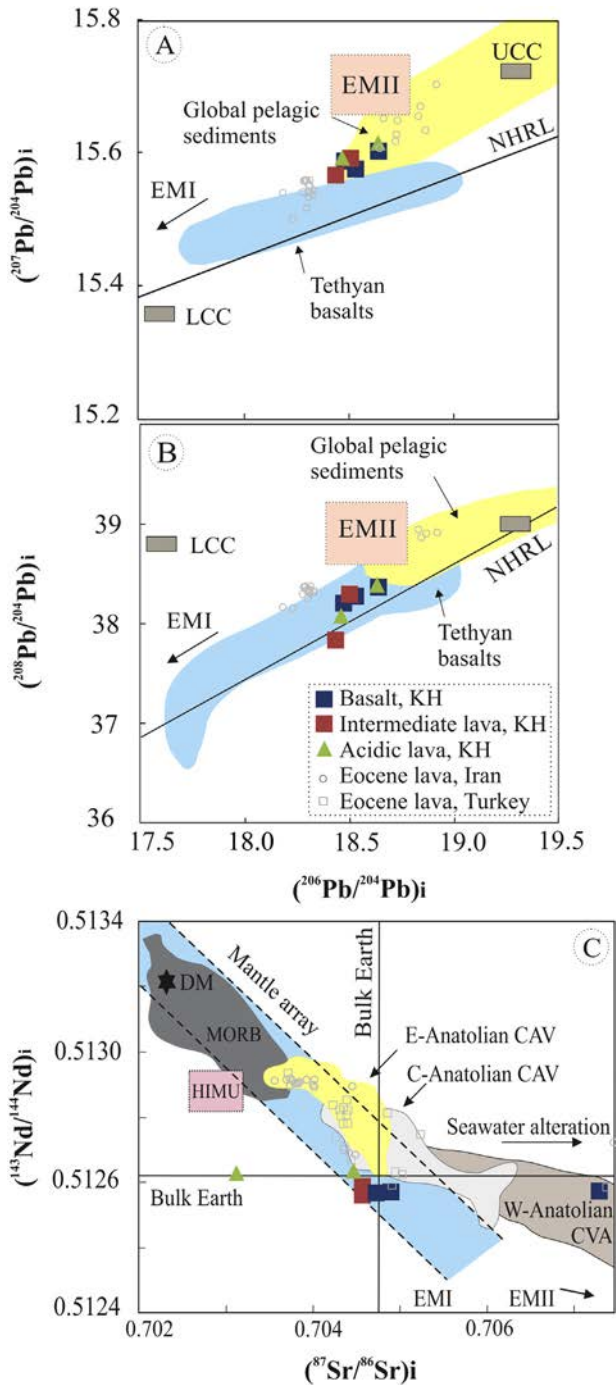
Fig. 7. (A) $^{206}Pb/^{204}Pb_i$ versus $^{207}Pb/^{204}Pb_i$ and (B) $^{208}Pb/^{204}Pb_i$ plots for the Kahrizak volcanic rocks. Data for Urumieh-Dokhtar are from Mirnejad et al. (2011), Eocene volcanic rocks for Sabzevar (SZ) are from Moghadam et al. (2016), Tethyan basalts and global pelagic sediments are from Ferguson and Klein (1993) and Pearce et al. (1995), Mariana Trough are from Straub and Zellmer (2012), and upper continental crust (UCC) and lower continental crust (LCC) are from Hofmann (1997). (C) $^{87}Sr/^{86}Sr_i$ versus $^{143}Nd/^{144}Nd_i$ plot for the Kahrizak volcanic rocks. Eocene lavas from Iran (Urumieh-Dokhtar from Omrani et al., 2008; Sabzevar from Moghadam et al., 2016; also gabbro in Sanandaj-Sirjan from Deevsalar et al., 2017), and from Turkey (Aydıncakır and Sen, 2013; Kaygusuz, 2009; Keskin et al., 2006; Kurt et al., 2008; Pamić et al., 1995; Pearce et al., 1990; Temizel et al., 2012; Varol et al., 2007) are shown for comparison. Fields for MORB and mantle array are from Wilson (1989) and McCulloch et al. (1994); proposed EMI, EMII, HIMU, and DM mantle end-members and bulk Earth compositions are from Zindler and Hart (1986), the Northern Hemisphere Reference Line (NHRL) is from Hart (1984), and the seawater alteration trend is from McCulloch et al. (1994). CAV = calc-alkaline volcanics. Two Kahrizak samples with very low $^{87}Sr/^{86}Sr_i$ are not plotted.

One way to illustrate the possible effects of the AFC process in the Kahrizak volcanic rocks is shown in Fig. 8E. The $^{87}Sr/^{86}Sr$ ratio versus Rb relationship of the Kahrizak basaltic and intermediate rocks defines a trend that is close to or parallels the straight line that links the composition of an enriched mantle source and a continental crust end-member (Scharer, 1991). Along this line, an AFC model is constructed using a value of $r = 0.4$ and $K_{d(Rb)} = 0.15$ for the mineral phases present in the basalts. This model indicates that the basalts are magmas coming from an enriched mantle and experience ca. 40% AFC with continental crust. Note that although some samples (one basalt and two rhyolites) plot far from the line, indicating their Rb and $^{87}Sr/^{86}Sr$ compositions are most probably altered, the overall trend of Kahrizak volcanic rocks still provides useful information on their petrogenesis.

In summary, geochemical and isotopic data indicating that fractional crystallization and assimilation of upper crust material have played an important role in the petrogenesis of the Kahrizak volcanic rocks.

5.2. Partial melting of the source

In this section, the concentrations of some fluid-immobile, incompatible trace elements (i.e., Ta, Th, Yb, Ti, and Nb) are used to constrain the relative degree of partial melting of the mantle source to produce the primary Kahrizak basaltic rocks (e.g., Gribble et al., 1996). In general, the moderately enriched REE patterns (Fig. 6B) and relatively low La/Lu_{Ch} (4–11) ratio of the Kahrizak basalts discount the role of garnet in their mantle source. The same is true for the Eocene arc volcanic rocks from northern Anatolia (Keskin et al., 2008), but not for those from the eastern Pontides (Temizel et al., 2012). Specifically, the Yb and TiO_2 compositions of Kahrizak basaltic rocks are consistent with the presence of spinel in their mantle source (Fig. 9A). Model calculations indicate that the Kahrizak basalts can be produced by about 10% to 30% partial melting of a spinel lherzolite, similar to that of the Mariana Trough basalts. The Th/Ta and Nb/Ta ratios of Kahrizak basalts also suggest a relatively high degree of partial melting at shallow depth (Fig. 9B). In detail, the Nb/Ta ratios, as proxy for degree of melting, of Kahrizak basalts are displaced toward high values similar to the rift basalts from the Mariana Trough at near-constant Th/Ta ratios (Nb/Ta = 12–19). Thus, alteration-resistant, incompatible trace element data suggest that the Kahrizak volcanics were produced by high degree of partial melting in the spinel stability field.

5.3. Nature of the magma source

As discussed above, major and trace elements and Nd and Pb isotope data suggest a common source for the pyroclastics and lava flows in the Kahrizak Mountains. In $^{206}Pb/^{204}Pb_i$ versus $^{208}Pb/^{204}Pb_i$ and $^{207}Pb/^{204}Pb_i$ plots (Fig. 7A, B), the Kahrizak volcanic rocks generally plot above the northern hemisphere reference line (NHRL) and toward the proposed enriched mantle II (EMII) mantle end-member (Zindler and Hart, 1986) as well as overlap with the field for global pelagic sediments (Ferguson and Klein, 1993). On the other hand, their depletion of Nb and Ta relative to LILEs can be attributed primarily to two processes: (1) addition of a LILE-enriched, but Nb and Ta poor subduction component to their mantle source or (2) assimilation of continental crust (Keskin et al., 2008). As also discussed above, assimilation of continental crust combined with fractional crystallization (AFC), plus alteration, may have played a role in generating the compositional variation of the Kahrizak volcanics, but these are clearly evident mainly in the differentiated rocks.

In general, many geochemical features of Kahrizak volcanic rocks, particularly the relatively more primitive basalts, indicate that they are associated with subduction. For example, higher Th/Ce, Nb/Zr and Th/Nb ratios and lower Pb/Nd ratios in high-Al arc magmas relative to MORB are commonly interpreted as the result of sediment input into their mantle source (e.g., Gertisser and Keller, 2003). The Kahrizak
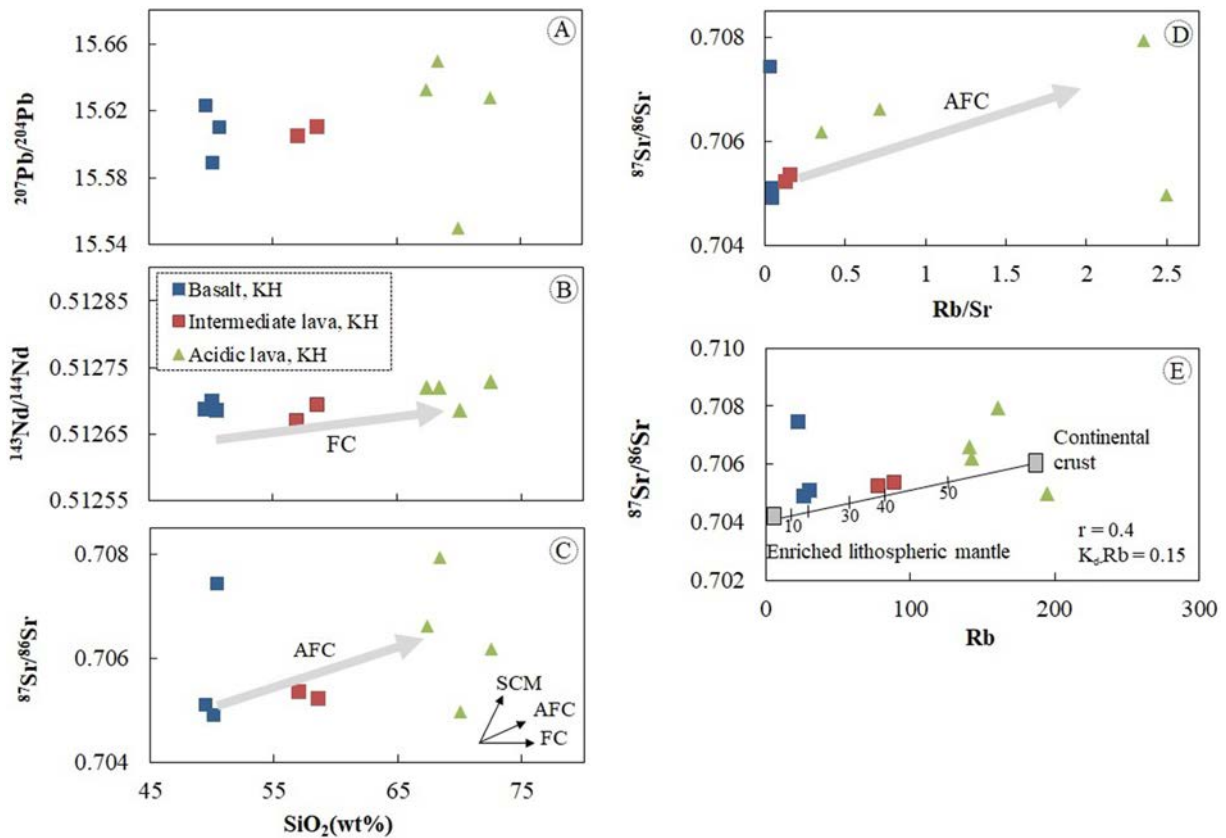
Fig. 8. (A) Measured $^{207}Pb/^{204}Pb$, (B) $^{143}Nd/^{144}Nd$ and (C) $^{87}Sr/^{86}Sr$ versus SiO_2 (wt%) plots for the Kahrizak volcanic rocks showing possible fractional crystallization (FC) and assimilation-fractional crystallization (AFC) trends (SCM = subcontinental mantle). (D) measured $^{87}Sr/^{86}Sr$ versus Rb/Sr and (E) Rb plots for the Kahrizak volcanic rocks. Solid line represents mixing between enriched SCLM composition and continental crust from Scharer (1991). Numbers next to the mixing line correspond to % contribution from sediments. Bulk rock Rb partition coefficient (K_d) value used in the AFC model was calculated from individual mineral partition coefficient values from the GERM Partition Coefficient (K_d) Database (https://earthref.org/KDD/).

volcanic rocks display relatively high Al_2O_3 contents (14.18–21.5 wt%), Th/Ce (0.02–0.57), Nb/Zr (0.06–0.22) and Th/Nb (0.05–1.64) ratios, and low Pb/Nd (0.09–0.71) ratios, which indeed suggest the involvement of subducted sedimentary materials in their magma source, as is proposed for eastern Pontides (Aydıncakır and Sen, 2013; Temizel et al., 2012). The elevated P content of Kahrizak basalts ($P_2O_5 = 0.3–1.0\%$) can also be explained by the presence of sediment in their source (Raos and Crawford, 2004).

The source enrichment features in the Kahrizak volcanic rocks can be constrained through a plot of Th/Yb versus Ta/Yb (Fig. 10), as these

elemental ratios can be effectively used to display source variation and crustal contamination (Pearce et al., 1990). In the plot, the Kahrizak volcanic rocks have high Th/Yb for given Ta/Yb ratios, suggesting they were derived from a mantle source containing a subduction component. Significantly, the trachydacites and rhyolites have Ta/Yb values that indeed plot along lines for AFC and mixing with continental crust, consistent with the earlier discussion. In comparison, volcanic rocks from eastern Pontides, northern Anatolia and UDA exhibit elongated fields that are subparallel to the mantle metasomatism array. Thus, the geochemical characteristics of Kahrizak basaltic rocks were likely inherited from a
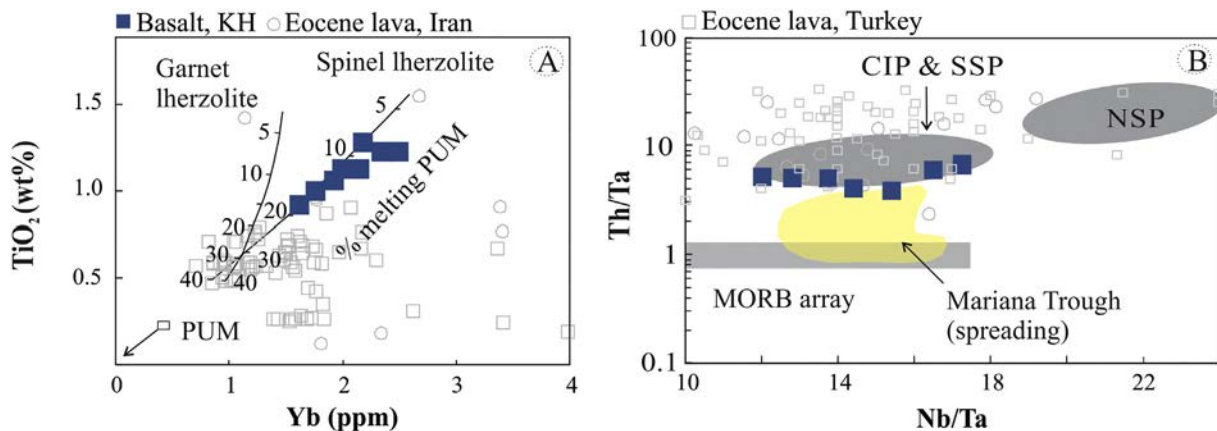

Fig. 9. Plots to estimate the degrees of partial melting that generated the Kahrizak basalts. (A) Ti versus Yb with a fixed primitive upper mantle (PUM) composition (Gribble et al., 1996). This plot assumes that the Mariana Trough backarc basin basalts (BABB) were produced by 6% to 24% partial melting in the spinel lherzolite stability field, with the highest value of 34% representing an arc-like basalt (Pearce and Stern, 2006). (B) Th/Ta (a proxy for the deep subduction component) versus Nb/Ta (a proxy for degree of melting and mantle depletion). Central and southern Mariana arcs = CIP and SSP, respectively and northern Mariana arc = NSP. See text for discussion.
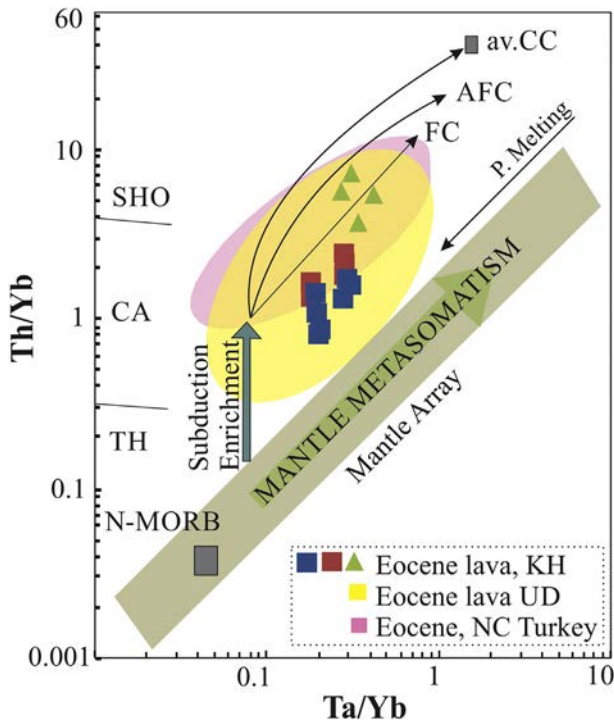
Fig. 10. Th/Yb versus Ta/Yb diagram (after Pearce et al., 1990) for the Kahrizak volcanic rocks. Average continental crust = av. CC from Taylor and McLennan (1985). Data for Urumieh-Dokhatr are from Omrani et al. (2008) and Verdel et al. (2011); those from Turkey are from Aydıncakır and Sen (2013), Temizel et al. (2012) and Keskin et al. (2008). See text for discussion.

mantle source that had been metasomatized by a subduction component. Correlatively, the low Nb/La and Ce/Pb ratios of the Kahrizak volcanics (Fig. 11A, B) indicate the influence of fluids dehydrated from subducted slab. Altogether these data suggest that the Kahrizak primary magmas were derived by partial melting of a mantle that had been metasomatized by fluids enriched with subduction component. However, this brings the question regarding the true or original nature of the mantle that was metasomatized by the subduction fluids.

Fig. 11B also clearly shows that although the Th/La ratio of Kahrizak rhyolitic lavas has a bulk upper crust affinity, the basaltic lavas have a Th/La ratio that is higher than that of MORB (Plank, 2005). Moreover, the Kahrizak volcanic rocks have a limited and low range of $^{143}Nd/^{144}Nd_i$ and most of the basaltic rocks have sub-bulk silicate Earth $^{86}Sr/^{87}Sr_i$ (Fig. 7C). These values are within the field of sublithospheric mantle (e.g., Arndt, 2013; Farmer, 1988). In addition, Eocene volcanic rocks that occur in almost all of Central Iran and

adjacent Urumieh-Dokhtar and Sanandaj-Srjan provinces have a compositional range that is highly consistent with a lithospheric mantle source (Keskin et al., 2008; Pearce et al., 1990; Temizel et al., 2012). Consequently, the parental magmas of the Kahrizak volcanic rocks were most probably derived from a lithospheric mantle source that was subsequently enriched by fluids produced during earlier subduction events; the magmas further experienced AFC during ascent to the surface. The parental magmas were produced by moderately high degree of partial melting from such enriched lithospheric mantle source at a shallower depth (probably temperature <900 °C according to Fig. 4A, B) and possess the isotopic and elemental signatures that are commonly observed in north-central Iran and surrounding regions.

5.4. Implications for the geodynamic evolution of north-Central Iran and surrounding areas

The Kahrizak Mountain volcanism is part of the Eocene magmatic flare-up in Central Iran, eastern Pontides and northern Anatolia. A variety of mechanisms have been proposed to explain the origin of the flare-up. These include volcanism related to subduction (Berberian and Berberian, 1981; Shahabpour, 2007), slab-melting (Ghorbani and Bezenjani, 2011), rifting and back-arc magmatism (Emami, 1981; Kazmin et al., 1986), slab break-off (e.g., Hassanzadeh et al., 2009; Jahangiri, 2007), and, lately, extensional arc flare-up due to slab rollback following a period of flat-slab subduction (Verdel et al., 2011; Zhang et al., 2018). Among these proposals, we find that the slab rollback scenario of Verdel et al. (2011) is most consistent with our data and literature data on Eocene magmatism, as summarized below. (1) The magmatism covers a wide area and was initiated prior to the Arabian-Eurasia continental collision. (2) It was temporally restricted to a ca. 17 Myr period. (3) Despite variations, the magmas overall have arc-like geochemical characteristics. (4) There is a trend in some localities for the magma composition to be initially calc-alkaline and, then, to be alkaline and shoshonitic.

Verdel et al.'s proposed mechanism is a four-stage model that started with a pre-conditioning of the arc lithosphere due to steep slab descent, followed by the spread of the pre-conditioning due to the Cretaceous flattening of the slab in the second stage. It was during the third stage that the Eocene volcanic rocks having major and trace element characteristics that are typical of continental arc magmatism were erupted. The magmas came from the decompression melting of the subduction-preconditioned arc lithospheric mantle or subcontinental lithospheric mantle (SCLM) due to lithospheric extension and crustal thinning accompanying slab rollback. Extension continued during the fourth stage in late Oligocene to Miocene, and the flare-up ended when the supply of preconditioned SCLM was exhausted, and replaced by asthenosphere-derived, OIB-type volcanism.
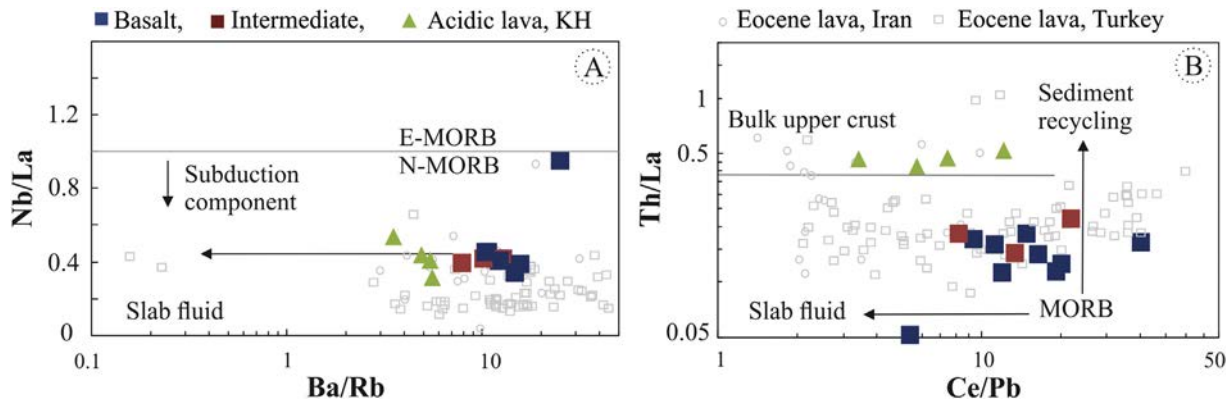

Fig. 11. (A) Nb/La versus Ba/Rb (N-MORB and E-MORB values are from Wang et al., 2004) and (B) Th/La versus Ce/Pb (reference ratio for Th/La from Plank, 2005; Ce/Pb reference ratio from Wang et al., 2004) diagrams for the Kahrizak volcanic rocks. See text for discussion.

We also concur that one of the key aspects of the appropriate mechanism is extensive preconditioning of the SCLM, but we want to emphasize that the preconditioning process most likely predated the 50 Myr flat-slab subduction (Verdel et al., 2011). The region experienced the subduction of the Neo-Tethys slab from at least the Early Jurassic until late Oligocene. The long-term subduction underneath Central Iran greatly affected the composition of the region's SCLM and asthenosphere, portions of which were trapped or wedged between subducting slabs and overlying plates. Fluids from the subducting slabs metasomatized the SCLM and the mantle wedges, which, as is typical along convergent margins, were the sources of arc magmas erupted in various parts of the region. As the Neo-Tethys closed, subduction slowed down and this may have increased the effectiveness of mantle fertilization (Verdel et al., 2011).

The uppermost asthenosphere and particularly the SCLM may have indeed partially melted due to decompression during lithospheric extension and crustal thinning (Verdel et al., 2011). However, the SCLM also could have been thermally perturbed because of the partial removal of its lithospheric root either by delamination or detachment of subducted slab (Bottrill et al., 2012; Pearce et al., 1990; Temizel et al., 2012). In general, magmas formed during the flare-up were dominated by basaltic melts from the metasomatized SCLM. Some of these magmas, however, assimilated crustal mineral while fractional crystallization was taking place to produce the rhyolitic high K-calc-alkaline to shoshonitic lavas. The assimilation process became more pronounced toward the end of the flare-up when magmatic input from the SCLM decreased and asthenosphere-derived, OIB-type magmas were added (Verdel et al., 2011). The end of the flare-up occurred during the 'soft' Arabia-Eurasia collision that is commonly estimated to be in late Eocene (Bottrill et al., 2012), although arc and associated extensional magmatism continued until late Oligocene to Miocene (Verdel et al., 2011; Zhang et al., 2018). Thus, partial melting of metasomatized lithospheric mantle accompanied by assimilation of the crust generated the Eocene calc-alkaline to high-k calc-alkaline and shoshonitic basaltic to rhyolitic rocks in north-central Iran and surrounding areas (see also, e.g., Temizel and Arslan, 2008, 2009).

6. Conclusions

(1) The Kahrizak Mountains in north-central Iran generally consists of Eocene basaltic to rhyolitic lavas interbedded with pyroclastic deposits formed in a shallow marine environment. The lavas include basalt, basaltic trachyandesite/andesite, trachydacite and rhyolite that can be classified into calc-alkaline basaltic group and high K-calc-alkaline to shoshonitic trachydacite-rhyolite group. The petrography of the volcanic rocks shows evidence of mineral-melt disequilibria.

(2) Despite some evidence of alteration, major and trace element variations indicate a general increase in incompatible trace elements with differentiation, consistent with the effects of fractional crystallization. The disequilibrium textures and complex compositional variations of minerals and other geochemical data are consistent with contamination or assimilation of crustal rocks. Overall, trace element variations suggest that the volcanic rocks in north-central Iran were derived from a relatively enriched lithospheric mantle source and had assimilated continental crust materials.

(3) The distinct enrichment in LILE and to a lesser extent in light REE, but depletion in HFSE of the lavas are similar to those of Paleogene volcanic rocks in eastern Pontides (northeastern Turkey) and northern Anatolia (north-central Turkey). Moreover, the rhyolitic rocks have compositional similarities with the upper crust.

(4) The basaltic rocks have a narrow range of initial Pb and Nd isotopic composition that indicates a common, fairly homogeneous source. However, the measured Sr, Pb and, to a certain extent,

Nd isotopic ratios correlate with degree of differentiation; these suggest an additional enriched component was involved in the petrogenesis of the volcanic rocks.

(5) Data indicate that the original source of the basaltic magmas was the lithospheric mantle that was previously metasomatized by fluids derived from the subducted oceanic slabs. Partial melting of such a source produced the bulk of the calc-alkaline basaltic group. Assimilation of continental crust and mixing with the basaltic magmas produced the intermediate to rhyolitic group.

(6) The Eocene volcanic rocks in north-central Iran and surrounding areas were derived through partial melting of the subduction-preconditioned subcontinental lithospheric mantle and asthenosphere during extension and thinning of the lithosphere at the waning stages of the closing of the Neo-Tethys Ocean.

References

Afaghi, A., Afshar, A., Jalilian, M., Ghandchi, M., Kamali, Gh., 1986. 1/250,000 Map of Tehran. Geological Survey of Iran.

Agard, P., Omrani, J., Jolivet, L., Whitechurch, H., Vrielynck, B., Spakman, W., Monie, P., Meyer, B., Wortel, R., 2011. Zagros orogeny: a subduction-dominated process. Geological Magazine 148, 692–725.

Alagna, E.K., Peccerillo, A., Martin, S., Carmelita Donati, C., 2010. Tertiary to present Evolution of Orogenic Magmatism in Italy. Journal of the Virtual Explorer 36, 1–18.

Amidi, S.M., Emami, M.H., Michel, R., 1984. Alkaline character of Eocene volcanism in the middle part of Central Iran and its geodynamic situation. Geologische Rundschau 73, 917–932.

Armstrong, J.T., 1995. CITZAF: a package of correction programs for the quantitative electron microbeam X-ray analysis of thick polished materials, thin films, and particles. Microbeam Analysis Journal 4, 177–200.

Arndt, N.T., 2013. Formation and evolution of the continental crust. Geochemical Perspectives (3), 1–533.

Aydıncakır, E., Sen, C., 2013. Petrogenesis of the post-collisional volcanic rocks from the Borçka (Artvin) area: Implications for the evolution of the Eocene magmatism in the Eastern Pontides (NE Turkey). Lithos 172-173.

Berberian, F., Berberian, M., 1981. Tectono-plutonic episodes in Iran in Zagros, Hindu Kush, Himalaya. Geodynamic Evolution 5–32.

Berberian, M., King, G.C.P., 1981. Towards a paleogeography and tectonic evolution of Iran. Canadian Journal of Earth Sciences 18, 210–265.

Bottrill, D., Van Hunen, J., Allen, M.B., 2012. Insight into collision zone dynamics from topography: numerical modelling results and observations. Solid Earth 3, 387–399.

Castillo, P.R., 2012. Adakite petrogenesis. Lithos 134-135, 304–316.

Castillo, P.R., Janney, P.E., Solidum, R.U., 1999. Petrology and geochemistry of Camiguin Island, southern Philippines: insights to the source of adakites and other lavas in a complex arc setting. Contributions to Mineralogy and Petrology 134, 33–51.

Davidson, J.P., Turner, S., Plank, T., 2013. Dy/Dy*:Variations arising from mantle sources and petrogenetic processes. Journal of Petrology 54, 525–537.

Deevsalar, R., Shinjo, R., Ghaderi, M., Murata, M., Hoskin, P.W.O., Oshiro, S., Neill, I., 2017. Mesozoic–Cenozoic mafic magmatism in Sanandaj–Sirjan Zone, Zagros Orogen (Western Iran): Geochemical and isotopic inferences from Middle Jurassic and late Eocene gabbros. Lithos 284–285, 588–607.

Draper, D.S., Johnston, A.D., 1992. Anhydrous PT phase relations of an Aleutian high-MgO basalt; an investigation of the role of olivine-liquid reaction in the generation of arc high-alumina basalts. Contributions to Mineralogy and Petrology 112, 501–519.

Elkins, L.T., Grove, T.L., 1990. Ternary feldspar experiments and thermodynamic models. American Mineralogist 75, 544–559.

Emami, M.H., 1981. Géologie de la région de Qom-Aran (Iran). Contribution à l'étude dynamique et géochimique du volcanisme tertiaire de l'Iran Central. Thèse Doctorat Etat. Grenoble, p. 489.

Farmer, G.L., 1988. Isotope geochemistry of mesozoic and tertiary igneous rocks in the Western United States and implications for the structure and composition of the deep continental lithosphere. In: Ernst, G. (Ed.), Metamorphism and Crustal Evolution in the Western United States, Rubey. Vol. 7. Prentice-Hall, Englewood Cliffs, New Jersey, pp. 87–109.

Ferguson, E.M., Klein, E.M., 1993. Fresh basalts from the Pacific– Antarctic Ridge extend the Pacific geochemical province. Nature 366, 330–333.

Gertisser, R., Keller, J., 2003. Trace element and Sr, Nd, Pb and O isotope variations in medium-K and high-K volcanic rocks from Merapi Volcano, Central Java, Indonesia: evidence for the involvement of subducted sediments in Sunda Arc magma genesis. Journal of Petrology 44, 457–489.

Ghorbani, M.R., Bezenjani, R.N., 2011. Slab partial melts from the metasomatizing agent to adakite, Tafresh Eocene volcanic rocks, Iran. Island Arc 20, 188–202.

Gribble, R.F., Stern, R.J., Bloomer, S.H., Stuben, D., O'Hearn, T., Newman, S., 1996. MORB mantle and subduction components interact to generate basalts in the southern Mariana Trough back-arc basin. Geochimica Cosmochimica Acta 60, 2153–2166.

Hart, S.R., 1984. A large scale isotopic anomaly in the southern hemisphere mantle. Nature 309, 753–757.

Hassanzadeh, J., Wernicke, B.P., 2016. The Neotethyan Sanandaj-Sirjan zone of Iran as an archetype for passive margin-arc transitions. Tectonics 35, 586–621.

Hassanzadeh, J., Stockli, D.F., Horton, B.K., Axen, G.J., Stockli, L.D., Grove, M., Schmitt, A.K., Walker, J.D., 2008. U-Pb zircon geochronology of late Neoproterozoic-early Cambrian granitoids in Iran: Implications for paleogeography, magmatism, and exhumation history of Iranian basement. Tectonophysics 451, 71–96.

Hassanzadeh, J., Wernicke, B.P., Ghazi, A.M., 2009. Timing of Arabia-Eurasia collision in Iran constrained by post-collisional magmatism. Geology Society of America. Abstract 41, 407.

Hawthorne, F.C., 1983. The chemistry of the amphiboles. Canadian Mineralogist 21, 173–480.

Hofmann, A.W., 1997. Mantle geochemistry: the message from oceanic volcanism. Nature 385, 219–229.

Horton, B.K., Hassanzadeh, J., Stockli, D.F., Axen, G.J., Gillis, R.J., Guest, B., Amini, A., Fakhari, M.D., Zamanzadeh, S.M., Grove, M., 2008. Detrital Zircon Provenance of Neoproterozoic to Cenozoic Deposits in Iran: Implications for Chronostratigraphy and Collisional Tectonics. vol. 451 pp. 97–122.

Hosseini, M.R., Hassanzadeh, J., Alirezaei, S., Sun, W., Li, C.Y., 2017. Age revision of the Neotethyan arc migration into the southeast Urumieh-Dokhtar belt of Iran: Geochemistry and U–Pb zircon geochronology. Lithos 284-285, 296–309.

Irvine, T.N., Baragar, W.R.A., 1971. A guide to the chemical classification of the common volcanic rocks. Canadian Journal of Earth Sciences 8, 523–548.

Jahangiri, A., 2007. Post-collisional Miocene adakitic volcanism in NW Iran: Geochemical and geodynamic implications. Journal of Asian Earth Science. 30, 433–447.

James, D.E., 1982. A combined O, Sr, Nd, and Pb isotopic and trace element study of crustal contamination in central Andean lavas, I. Local geochemical variations. Earth and Planetary Science Letters 57, 47–62.

Kaygusuz, A., 2009. K/Ar ages and geochemistry of the collision related volcanic rocks in the Ilıca (Erzurum) area, eastern Turkey. Neues Jahrbuch für Mineralogie 186, 21–36.

Kazmin, V.G., Sbortshikov, I.M., Ricou, L.E., Zonenshain, L.P., Boulin, J., Knipper, A.L., 1986. Volcanic belts as markers of the Mesozoic- Cenozoic active margin of Eurasia. Tectonophysics 123, 123–152.

Keskin, M., Pearce, J.A., Kempton, P.D., Greenwood, P., 2006. Magma-crust interactions and magma plumbing in a postcollisional setting: Geochemical evidence from the erzurum-kars volcanic plateau, Eastern Turkey. In: Dilek, Y., Pavlides, S. (Eds.), Postcollisional Tectonics and Magmatism in the Mediterranean Region and Asia. Geological Society of America, pp. 475–505.

Keskin, M., Can Genç, S., Tüysüz, O., 2008. Petrology and geochemistry of post-collisional Middle Eocene volcanic units in North-Central Turkey: evidence for magma generation by slab breakoff following the closure of the Northern Neotethys Ocean. Lithos 104, 267–305.

Kheirkhah, M., Allen, M.B., Emami, M., 2009. Quaternary syn-collision magmatism from the Iran/Turkey borderlands. Journal of Volcanology and Geothermal Research 182, 1–12.

Kurt, H., Asan, K., Ruffet, G., 2008. The relationship between collision-related calcalkaline, and within-plate alkaline volcanism in the Karacadağ area (Konya-Türkiye, Central Anatolia). Chemie Der-Erde Geochemistry 68, 155–176.

Le Bas, M.J., Le Maitre, R.W., Streckeisen, A., Zannetin, B., 1986. A chemical classification of volcanic rocks based on the total alkali- silica diagram. Journal Petrol 27, 745–750.

Mattioli, M., Renzulli, A., Menna, M., Holm, P.M., 2006. Rapid ascent and contamination of magmas through the thick crust of the CVZ (Andes, Ollagüe region): evidence from a nearly aphyric high-K andesite with skeletal olivines. Journal of Volcanology and Geothermal Research 158, 87–105.

McCulloch, M.T., Kyser, T.K., Woodhead, J.D., Kinsley, L., 1994. Pb-Sr-Nd-O Isotopic Constraints on the Origin of Rhyolites from the Taupo Volcanic Zone of New Zealand: evidence for Assimilation followed by Fractionation of Basalt. Contributions to Mineralogy and Petrology 115, 303–312.

Mirnejad, H., Simonetti, A., Molasalehi, F., 2011. Pb isotopic compositions of some Zn–Pb deposits and occurrences from Urumieh–Dokhtar and Sanandaj–Sirjan zones in Iran. Ore Geology Reviews 39, 181–187.

Moghadam, H.S., Rossetti, F., Lucci, F., Chiaradia, M., Gerdes, A., Martinez, M.L., Ghorbani, G., Nasrabady, M., 2016. The Calc-alkaline and adakitic volcanism of the sabzevar structural zone (NE Iran): Implications for the eocene magmatic flare-up in Central Iran. Lithos 248–251, 517–535.

Morimoto, N., 1988. Nomenclature of Pyroxenes. Mineralogy and Petrology 39, 55–76.

Nelson, S.T., Montana, A., 1992. Sieve-textured plagioclase in volcanic rocks produced by rapid decompression. American Mineralogist 77, 1242–1249.

Omrani, J., Agard, P., Whitechurch, H., Benoit, M., Proutea, G., Jolivet, L., 2008. Arc-magmatism and subduction history beneath the Zagros Mountains, Iran: a new report of adakites and geodynamic consequences. Lithos 106, 380–398.

Pamić, J., McKee, E.H., Bullen, T.D., Lanphere, M.A., 1995. Tertiary Volcanic Rocks from the Southern Pannonian Basin, Croatia. International Geology Review 37, 259–283.

Pearce, J.A., Stern, R.J., 2006. Origin of Back-arc basin magma: Trace element and isotope perspectives. AGU Geophysical Monograph Series 166, 63–86.

Pearce, J.A., Bender, J.F., De Long, S.E., Kidd, W.S.F., Low, P.J., Guner, Y., Saroglu, F., Yilmaz, Y., Moorbath, S., Mitchel, J.G., 1990. Genesis of collision volcanism in Eastern Anatolia, Turkey. Journal of Volcanology and Geothermal Research 44, 189–229.

Pearce, J.A., Ernewein, M., Bloomer, S.H., Parson, L.M., Murton, B.J., Johnson, L.E., 1995. Geochemistry of Lau Basin volcanic rocks: influence of ridge segmentation and arc proximity. Geological Society London Special Publications 81, 53–75.

Pecerillo, A., Taylor, S.R., 1976. Geochemistry of Eocene calc-alkaline volcanic rocks from the Kastamonu area, Northern Turkey. Contributions to Mineralogy and Petrology 58, 63–81.

Pirouz, P., Avouac, J.P., Hassanzadeh, J., Kirschvink, J.L., Bahroudi, A., 2017. Early Neogene foreland of the Zagros, implications for the initial closure of the Neo-Tethys and kinematics of crustal shortening. Earth and Planetary Science Letters 477, 168–182.

Plank, T., 2005. Constraints from Thorium/Lanthanum on sediment recycling at subduction zones and the evolution of the continents. Journal of Petrology 46, 921–944.

Rahmati-Ilkhchi, M., Faryad, S.W., Holub, F.V., Kos'ler, J., Frank, W., 2011. Magmatic and metamorphic evolution of the Shotur Kuh metamorphic complex (Central Iran). Int J Earth Sci (Geol Rundsch) 100, 45–62.

Ramezani, J., Tucker, R.D., 2003. The Saghand region, Central Iran: U-Pb geochronology, petrogenesis and implications for Gondwana tectonics. American Journal of Science 303, 622–665.

Raos, A.M., Crawford, A.J., 2004. Basalts from the Efate Island Group, central section of the Vanuatu arc, SW Pacific: geochemistry and petrogenesis. Journal of Volcanology and Geothermal Research 134, 35–36.

Rossel, P., Oliveros, V., Mescua, J., Tapia, F., Ducea, N.M., Calderón, S., Charrier, R., Hoffman, D., 2014. The Upper Jurassic volcanism of the Río Damas-Tordillo Formation (33°-35.5°S): Insights on petrogenesis, chronology, provenance and tectonic implications. Andean. Geology 41, 529–557.

Rudnick, R.L., Gao, S., 2003. Composition of the continental crust. Treatise on Geochemistry 3, 1–64.

Sakuyama, M., 1979. Evidence of magma mixing: petrological study of Shirouma-Oike calc-alkaline andesite volcano, Japan. Journal of Volcanology Geothermal Research 5, 179–208.

Scharer, U., 1991. Rapid continental crust formation at 1.7 Ga from a reservoir with chondritic isotope signatures, eastern Labrador. Earth and Planetary Science Letters 102, 110–133.

Schiano, P., Monzier, M., Eissen, J.P., Martin, H., Koga, K.T., 2010. Simple mixing as the major control of the evolution of volcanic suites in the Ecuadorian Andes. Contributions to Mineralogy Petrology 160, 297–312.

Shahabpour, J., 2007. Island-arc affinity of the central Iranian volcanic belt. Journal of Asian Earth Sciences 30, 652–665.

Straub, M.S., Zellmer, G.F., 2012. Volcanic arcs as archives of plate tectonic change. Gondwana Research 21, 495–516.

Sun, S.S., McDonough, W.F., 1989. Chemical and isotopic systematic of oceanic basalts: Implication for mantle composition and processes. In: Rollinson, H.R. (Ed.), Using Geochemical Data: Evaluation, Presentation, Interpretation. John Wiley and Sons, p. 325.

Tatsumi, Y., Eggins, S.M., 1995. Subduction Zone Magmatism. Blackwell, Cambridge.

Taylor, S.R., McLennan, S.M., 1985. The Continental Crust; its Composition and Evolution. Blackwell Scientific, Oxford, Londan, Edinburgh, Boston, Palo Alto, Melbourne.

Temizel, İ., Arslan, M., 2008. Petrology and geochemistry of Tertiary volcanic rocks from the İkizce (Ordu) area, NE Turkey: Implications for the evolution of the eastern Pontide paleo-magmatic arc. Journal of Asian Earth Sciences 31, 439–463.

Temizel, İ., Arslan, M., 2009. Mineral chemistry and petrochemistry of post-collisional Tertiary mafic to felsic cogenetic volcanics in the Ulubey (Ordu) area, eastern Pontides, NE Turkey. Turkish Journal of Earth Sciences 18, 29–53.

Temizel, I., Arslan, M., Ruffet, G., Peucat, J.J., 2012. Petrochemistry, geochronology and Sr–Nd isotopic systematics of the Tertiary collisional and post-collisional volcanic rocks from the Ulubey (Ordu) area, eastern Pontides, NE Turkey: Implications for extension-related origin and mantle source characteristics. Lithos 128, 126–147.

Tian, L., Castillo, P.R., Hawkins, J.W., Hilton, D.R., Hanan, B.B., Pietruszka, A.A., 2008. Major and trace element and Sr-Nd isotopes ignatures of the mantle beneath the Central Lau Basin: implications for the nature and influence of subduction components. Journal of Volcanology and Geothermal Research 178, 657–670.

Tsuchiyama, A., 1985. Dissolution kinetics of plagioclase in the melt of the system diopside-albite-anortite, and origin of dusty plagioclase in andesite. Contribution Mineral Petrology 89, 1–6.

Varol, E., Temel, A., Gourgaud, A., Bellon, H., 2007. Early Miocene 'adakite-like' volcanism in the Balkuyumcu region, Central Anatolia, Turkey: petrology and geochemistry. Journal of Asian Earth Sciences 30, 613–628.

Verdel, C., Brian, P.W., Hassanzadeh, J., Guest, B., 2011. A Paleogene Extensional Arc Flare-Up in Iran. p. 30.

Wang, K.L., Chung, S.L., O'Reilly, S.Y., Sun, S.S., Shinjo, R., Chen, C.H., 2004. Geochemical constraints for the genesis of post-collisional magmatism and the geodynamic evolution of the Northern Taiwan Region. Journal of Petrology 45, 975–1011.

Whitechurch, H., Omrani, J., Agard, P., Humbert, F., Montigny, R., Jolivet, L., 2013. Evidence for Paleocene–Eocene evolution of the foot of the Eurasian margin (Kermanshah ophiolite, SWIran) from back-arc to arc: Implications for regional geodynamics and obduction. Lithos 182–183, 11–32.

Wilson, M., 1989. Igneous Petrogenesis: A Global Tectonic Aproach. Unwin Hyman, London, p. 466.

Yazdani, S., Castillo, P., Day, J., 2014. The Geochemistry of Zeolites and Calc-Alkaline Rocks from North-Central Iran and its Implications to Fluid/Rock Interaction and Alteration, SIO Student Symposium. University of California, San Diego.

Zhang, Z., Wenjiao Xiao, W., Ji, W., Majidifard, M.R., Rezaeian, M., Talebian, M., Xiang, D., Chen, L., Wan, B., Ao, S., Esmaeil, R., 2018. Geochemistry, zircon U-Pb and Hf isotope for granitoids NW Sanandaj-Sirjan zone, Iran: Implications for Mesozoic-Cenozoic ep-

isodic magmatism during Neo-Tethyan lithospheric subduction. Gondwana Research https://doi.org/10.1016/j.gr.2018.04.002.

Zindler, A., Hart, S.R., 1986. Chemical geodynamics. Annual Review of Earth and Planetary Sciences 14, 493–571.